

Analysis of a Three-Dimensional Dielectric Mixture with Finite Difference Method

Kimmo Kärkkäinen, *Student Member, IEEE*, Ari Sihvola, *Senior Member, IEEE*, and Keijo Nikoskinen, *Senior Member, IEEE*

Abstract—The present paper reports the results of a numerical analysis of electric fields in random dielectric materials. The effective permittivity of a three-dimensional (3-D) dielectric mixture is calculated by the finite difference method. The results show the distribution of the effective permittivity of a mixture with different random inclusion positionings. New empirical mixing models are created as least squares approximations to fit the collection of numerical results. The calculated permittivity distribution is also compared with theoretical mixture models, showing that in case of clustered inclusions, the Bruggeman model is quite reasonable. On the other hand, if the inclusions in the mixture are separate, the results are closer to the Maxwell–Garnett model.

Index Terms—Effective permittivity, finite differences, mixing rules.

I. INTRODUCTION

MATERIALS encountered in geophysical applications of remote sensing are quite often inhomogeneous and complicated in structure. Certainly there are exceptions, like air and water, which may safely be considered uniform to the electromagnetic wave but such common materials as snow, sea ice, and soil are strongly inhomogeneous in their structure. Geoscience objects like natural and cultural vegetation constitute an even more difficult challenge for electromagnetic modeling.

In such cases, the number of degrees of freedom in the material description has to be decreased very much in order to be able to make a reasonable effort in treating the interaction problem between electromagnetic waves and such a complex material object. An important tool in such a simplification process is the concept of effective dielectric constant. The dielectric response of the complex original object is condensed into this macroscopic permittivity. Of course, such a homogenization approach has limitations of which the user needs to be aware. A crucial one is that the inhomogeneity to be averaged has to be of clearly smaller scale than the wavelength of the operating field.

In earlier papers [1] and [2], we presented a way to calculate numerically the effective dielectric constant of a two-dimensional (2-D) random mixture. The mixture was a two-component mixture with a homogeneous background in which parallel cylinders of another material were embedded in random

positions. One can find such 2-D mixture geometries in many places in nature but very often mixtures have variation in all three dimensions. In this paper we consider fully 3-D mixtures. Instead of cylinders we now model spheres embedded in random positions. Spherical inclusions are allowed to touch and overlap which means that complex cluster geometries can be formed.

The electrostatic potential in the mixture is calculated using the finite difference method. Because an infinitely large random mixture cannot be modeled we end the computation domain with periodic boundary conditions. It means that we are actually modeling a periodic material which has a period that includes many randomly placed inclusions. The electric potential generated by a homogeneous excitation field is calculated in the mixture. The effective permittivity of the mixture is determined by calculating the electrostatic field energy. Several samples are analyzed with different random inclusion distributions. Of course, every new simulation of the random medium is individually different even if they have the same volume proportions of the phases, and hence a variation is to be expected in the results.

We study both the mixtures with inclusion permittivity higher than the environment permittivity and vice versa. Empirical models based on the numerical results are created for both types of mixtures. The electric flux distribution in a 3-D mixture is illustrated as a cross-sectional view. Although the main attention in the study is on the mixtures allowing inclusion clustering, also mixtures with separate inclusions (i.e., no clustering) are studied.

II. THREE-DIMENSIONAL MIXING MODELS

The mixture under study consists of two dielectric components, of which one is treated as host, and the other as the inclusion phase. In the literature, many mixing models can be found for the effective dielectric permittivity of such a mixture. Some are presented here.

For the case of spherical inclusions, the prediction of the effective permittivity of the mixture ϵ_{eff} according to the Maxwell–Garnett mixing rule reads [3], [4]

$$\epsilon_{\text{eff}} = \epsilon_e + 3f\epsilon_e \frac{\epsilon_i - \epsilon_e}{\epsilon_i + 2\epsilon_e - f(\epsilon_i - \epsilon_e)}. \quad (1)$$

Here, spheres of permittivity ϵ_i are located randomly in a homogeneous environment (ϵ_e) and occupy a volume fraction f . Another famous mixing rule is the Bruggeman formula [5]

$$(1 - f) \frac{\epsilon_e - \epsilon_{\text{eff}}}{\epsilon_e + 2\epsilon_{\text{eff}}} + f \frac{\epsilon_i - \epsilon_{\text{eff}}}{\epsilon_i + 2\epsilon_{\text{eff}}} = 0. \quad (2)$$

Manuscript received June 20, 2000; revised November 21, 2000.

K. Kärkkäinen was with the Electromagnetics Laboratory, Helsinki University of Technology, FIN-02015 HUT, Espoo, Finland. He is now with the Department of Electrical and Computer Engineering, University of Victoria, Victoria, BC, V8W 3P6 Canada.

A. Sihvola and K. Nikoskinen are with the Electromagnetics Laboratory, Helsinki University of Technology, FIN-02015 HUT, Espoo, Finland.

Publisher Item Identifier S 0196-2892(01)03829-3.

The Bruggeman rule is also known as the Polder–van Santen formula [6]. The mixing approach presented in [7] collects dielectric mixing rules into one family

$$\frac{\epsilon_{\text{eff}} - \epsilon_e}{\epsilon_{\text{eff}} + 2\epsilon_e + \nu(\epsilon_{\text{eff}} - \epsilon_e)} = f \frac{\epsilon_i - \epsilon_e}{\epsilon_i + 2\epsilon_e + \nu(\epsilon_{\text{eff}} - \epsilon_e)}. \quad (3)$$

This formula contains a dimensionless parameter ν . For different choices of ν , the previous mixing rules are recovered: $\nu = 0$ gives the Maxwell–Garnett rule, $\nu = 2$ gives the Bruggeman formula, and $\nu = 3$ gives the Coherent potential [8] approximation.

Different mixing models predict different effective permittivity values for a given mixture. However, there are bounds that limit the range of the predictions. The loosest bounds are the so-called Wiener bounds [9]. These effective permittivity bounds are

$$\epsilon_{\text{eff},\text{min}} = \frac{\epsilon_i \epsilon_e}{f \epsilon_e + (1-f) \epsilon_i} \quad (4)$$

and

$$\epsilon_{\text{eff},\text{max}} = f \epsilon_i + (1-f) \epsilon_e. \quad (5)$$

These two cases correspond to capacitors that are connected in parallel or series in a circuit. It is worth noting also that these two cases are the effective permittivities from the mixing formulas with aligned ellipsoids, where the depolarization factors are 0 and 1, respectively. Note that the bounds retain the minimum and maximum character independently of the type of the mixture, i.e., (4) is the minimum for both $\epsilon_i > \epsilon_e$ and $\epsilon_i < \epsilon_e$. Also, (5) is the maximum for both cases.

III. NUMERICAL TECHNIQUES

A. Simulation Setup

The effective permittivity of a mixture is determined by calculating electrostatic fields in the mixture sample. The sample is under influence of a homogeneous electric field. The computational domain is restricted with periodic boundary conditions. The simulation setup can be seen in Fig. 1. The sample is composed of the host material and randomly positioned spherical inclusions. Clustering of inclusions is allowed which means that the inclusions can form connected sets when overlapping each other. In x - and y -directions the potential has an ordinary periodic boundary condition, i.e., the potential distributions on the opposite faces of the computation domain are exactly the same. Because the excitation field is polarized in the z -direction the potential on the upper face is a constant higher than on the lower face

$$\phi(X_{\text{max}}, y, z) = \phi(0, y, z) \quad (6)$$

$$\phi(x, Y_{\text{max}}, z) = \phi(x, 0, z) \quad (7)$$

$$\phi(x, y, Z_{\text{max}}) = \phi(x, y, 0) + U_0. \quad (8)$$

These boundary conditions mean that in the numerical calculations the opposite faces are connected directly to each other. If an inclusion is placed on the boundary its body is continued through the opposite boundary. Therefore every inclusion is modeled as a whole sphere.

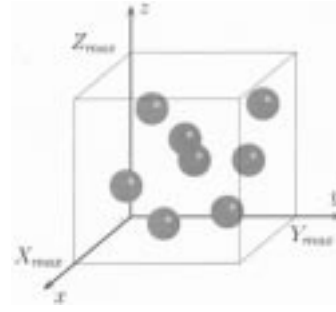


Fig. 1. Computation domain is one period of a periodic structure.

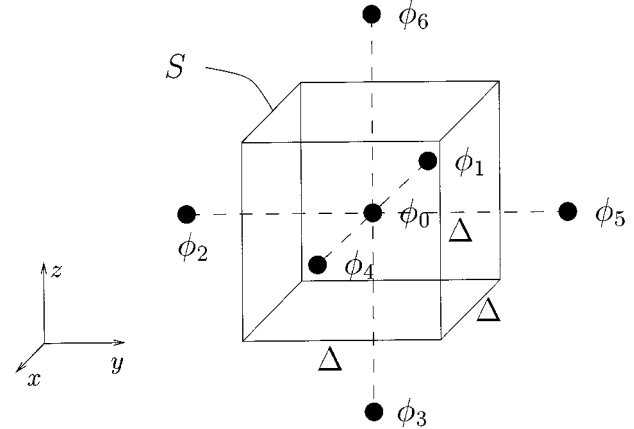


Fig. 2. Computation lattice.

B. Difference Equation for Potential

There are no free charges in an insulator medium. It means that the electric flux over an arbitrary closed boundary S surrounding the insulator medium is zero, i.e.,

$$\oint_S (\epsilon \nabla \phi) \cdot d\mathbf{S} = 0 \quad (9)$$

in which ϕ and ϵ are the electric potential and the permittivity. The whole insulator medium can be divided into small cubes. In every cube, (9) holds. Because the potential is defined in the center of each cube we can write the finite difference approximation for (9). The situation is illustrated in Fig. 2. In every face of a lattice cube the electric field is supposed to be linearly dependent of a spatial coordinate. Hence, the difference approximation of (9) is

$$\left(\epsilon_1 \frac{\phi_1 - \phi_0}{\Delta} + \epsilon_2 \frac{\phi_2 - \phi_0}{\Delta} + \epsilon_3 \frac{\phi_3 - \phi_0}{\Delta} + \epsilon_4 \frac{\phi_4 - \phi_0}{\Delta} + \epsilon_5 \frac{\phi_5 - \phi_0}{\Delta} + \epsilon_6 \frac{\phi_6 - \phi_0}{\Delta} \right) \Delta^2 = 0 \quad (10)$$

where ϵ_j are the effective permittivities of material between potentials ϕ_j and ϕ_0 . Equation(10) can be solved for the potential in the center of a lattice cube

$$\phi_0 = \frac{\sum_{j=1}^6 \epsilon_j \phi_j}{\sum_{j=1}^6 \epsilon_j}. \quad (11)$$

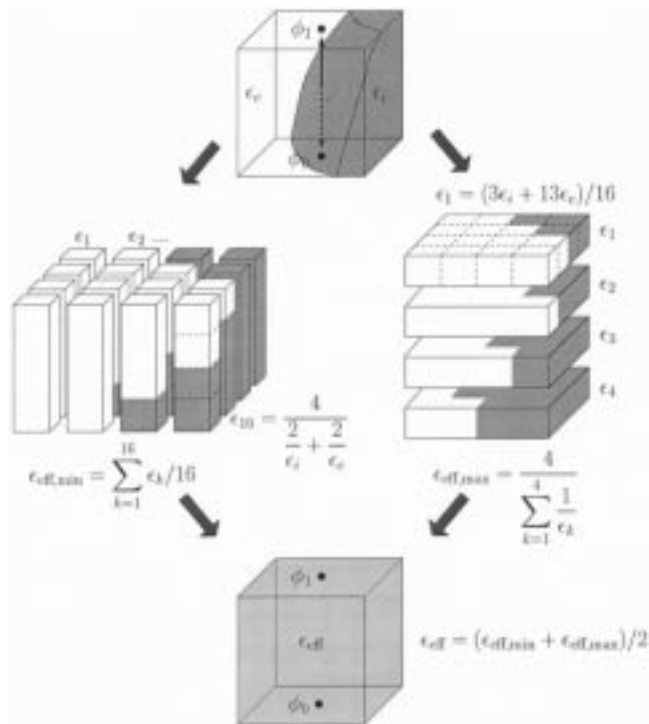


Fig. 3. Determination of effective permittivity between potential nodes near a material interface.

The Gauss-Seidel method with overrelaxation [10] is used to get an iterative solution for the potential. We get the following update equation:

$$\phi_0^{(n+1)} = \omega \frac{\sum_{j=1}^3 \epsilon_j \phi_j^{(n+1)} + \sum_{j=4}^6 \epsilon_j \phi_j^{(n)}}{\sum_{j=1}^6 \epsilon_j} + (1 - \omega) \phi_0^{(n)}. \quad (12)$$

The value of 1.95 was used for the overrelaxation coefficient ω .

The effective permittivity of a mixture is the permittivity value of homogenized material which gives same electrostatic energy as the studied mixture. Hence, effective permittivity can be calculated by approximating the integral

$$\epsilon_{\text{eff}} = \frac{Z_{\text{max}}}{U_0^2 X_{\text{max}} Y_{\text{max}}} \int_V \epsilon(\mathbf{r}) |\nabla \phi(\mathbf{r})|^2 dV \quad (13)$$

with a discrete sum over finite difference solution of potential.

C. Local Permittivity Near Material Interfaces

When the grid cell falls on a material interface, the permittivity value in the difference equation becomes ambiguous. In this analysis the local permittivity values ϵ_j between potential nodes are determined by the mixture geometry in the cubic volume element as shown in Fig. 3. This procedure gives the estimations of lower and upper limits for a local permittivity using the following reasoning.

Conjecture 1:

- If permittivity is locally decreased, the permittivity of the structure (here cubic element) is decreased or remains the same.
- If permittivity is locally increased, the permittivity of the structure is increased or remains the same.

To get the lower limit, we set material layers of zero permittivity parallel to the line connecting potential points. Hence we have a structure of parallel capacitors. For the upper limit estimation we set material layers of infinite permittivity perpendicular to the connecting line and we get a structure of capacitors in series. Finally the local permittivity between potential nodes is set to be an average of the lower and the upper limit. This is accurate for the cases in which the material interface is perpendicular or parallel to the connecting line. Naturally the technique does not give exact permittivity values for arbitrary oriented material surfaces. It is very difficult or maybe even an impossible task to determine effective permittivity value near arbitrary oriented surfaces. And one might doubt how just one number could represent the characteristics of material surface. Therefore it is reasonable to use mesh dense enough to clearly illustrate curved boundaries.

IV. RESULTS

A. Random Mixture

Effective permittivity was calculated for two types of mixtures: raisin pudding, where the inclusion permittivity is higher than the environment permittivity ($\epsilon_i > \epsilon_e$), and Swiss cheese, an inverted mixture, where the inclusion permittivity is lower than the environment permittivity ($\epsilon_i < \epsilon_e$). Inclusion and environment permittivity contrasts of

$$k = \frac{\epsilon_i}{\epsilon_e} = 2 + i^2, \quad i = 0, 1, \dots, 10 \quad (14)$$

were studied for the raisin pudding and $1/k$ for the Swiss cheese mixtures. The dependence of effective permittivity on inclusion volume fraction was studied in the whole range of $0 \dots 1$. This was possible because spherical inclusions were allowed to overlap. To characterize effective permittivity of random mixtures it was necessary to simulate a large group of mixture samples with random inclusion positionings. In every simulation, the inclusion volume fraction and positions of inclusions were randomly chosen. The computation domain size was $100 \times 100 \times 100 = 1\,000\,000$ cells. The diameter of an inclusion sphere was chosen to be 20 cells. It means that rather many inclusion balls did fit into the computation domain and still the description of a curved surface was reasonable accurate.

A distribution of simulation results for the permittivity contrast $k = 102$ can be seen in Fig. 4.

B. Empirical Mixing Model Based on the Numerical Results

One of the main interests of this study was to create a new mixing model with the help of calculated simulation results. The goal was to seek for a formula that gives a good fit to the set of over 4000 simulation results. In our earlier article [2] it was clarified for 2-D mixtures that the ν -model [7] with a constant ν cannot offer a good fit to numerical results in the whole range of inclusion volume fraction and permittivity contrast. This is also true for 3-D mixtures. However, if parameter ν is given a freedom to depend on both inclusion volume fraction and permittivity contrast ($k = \epsilon_i/\epsilon_e$) the model becomes much more flexible. Hence, by taking the ν -model as a basis

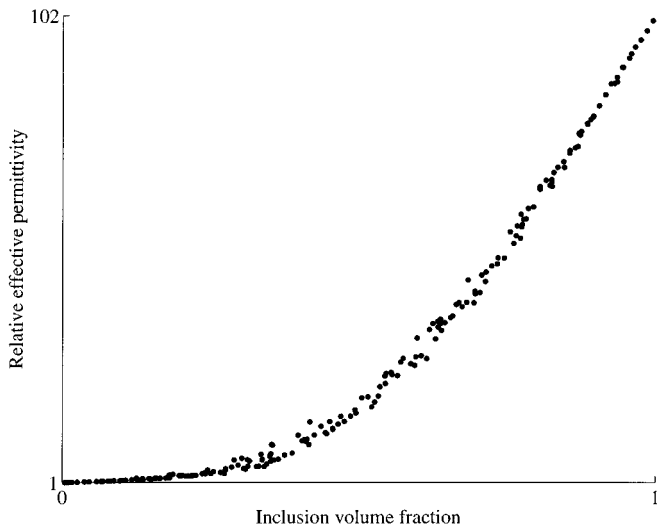


Fig. 4. Effective permittivity distribution of random mixtures ($k = 102$).

the fitting problem is now reduced to the problem of seeking for a function $\nu(f, k)$. ν was determined by least squares method for every calculated permittivity contrast as a function of inclusion volume fraction. After some studies it turned out that a second-order polynomial is good enough to describe the variation of ν in volume fraction direction. Therefore parameter ν is assumed to be of form

$$\nu(f, k) = a(k)f^2 + b(k)f + c(k). \quad (15)$$

Coefficients a , b , and c were determined for all permittivity contrasts calculated and it is noted that they are well represented by

$$a(k) = 1.27 + 1.43e^{-0.048k} \quad (16)$$

$$b(k) = -2.76 - 0.90e^{-0.043k} \quad (17)$$

$$c(k) = 2.35 \quad (18)$$

for the raisin pudding mixture in which $k > 1$ and

$$a(k) = 1.06 \quad (19)$$

$$b(k) = -1.23 + 0.44e^{-5.95k} \quad (20)$$

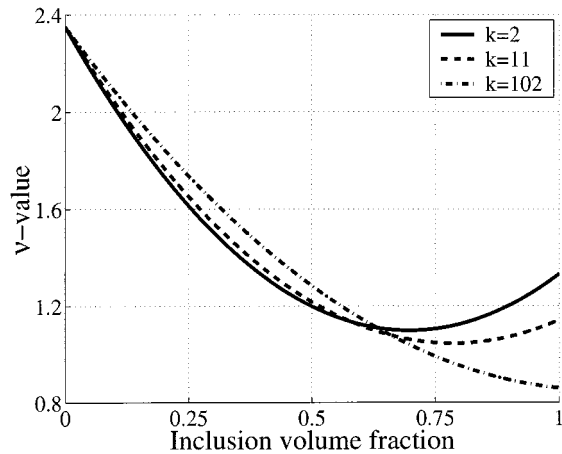
$$c(k) = 1.70 \quad (21)$$

for the Swiss cheese mixture in which $k < 1$. The proposed model based on the numerical results is therefore the model of (3) with parameter shown in

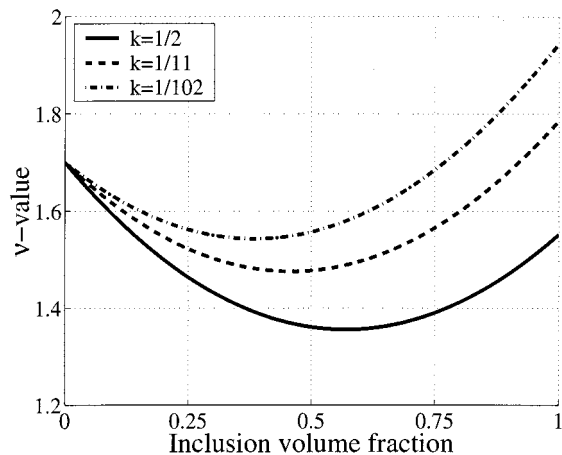
$$\nu(f, k) = \begin{cases} (1.27 + 1.43e^{-0.048k})f^2 \\ \quad + (-2.76 - 0.90e^{-0.043k})f + 2.35, & \text{if } k > 1 \\ 1.06f^2 \\ \quad + (-1.23 + 0.44e^{-5.95k})f + 1.70, & \text{if } k < 1. \end{cases} \quad (22)$$

The function values for some permittivity contrasts are plotted as a function of inclusion volume fraction in Fig. 5.

The validity of the model is of course restricted to the permittivity contrast values below 102. But the model is such that it does not give absurd values beyond this region either. This new model is plotted along with numerical results and theoretical mixing models in Figs. 6–8. At low volume fraction values the Bruggeman model agrees well with the simulated results.



(b)



(a)

Fig. 5. ν -values for the permittivity contrasts $k = 2, 11, 102$ and $k = 1/2, 1/11, 1/102$.

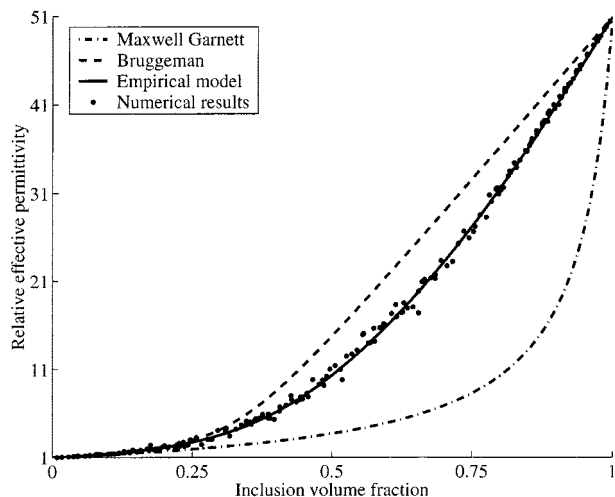


Fig. 6. Mixing models are plotted with numerical results for the raisin pudding mixture ($k = 51$).

C. Mixture Without Clustering

In many practical mixtures inclusions can be solid material and therefore they do not overlap and form clusters. With the introduced technique it is possible to model also these kind of mixtures. However, the range of inclusion volume fraction must

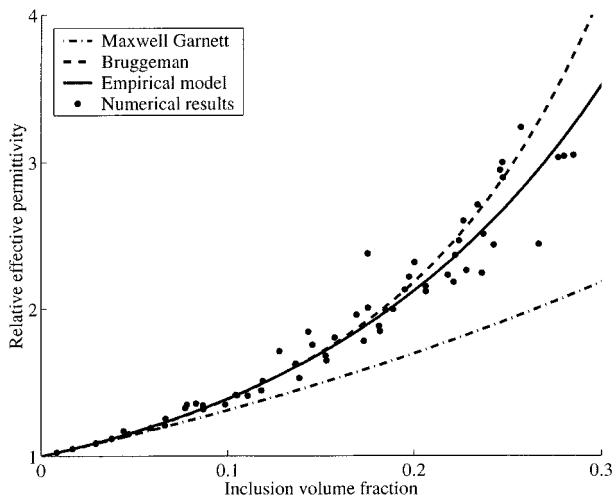


Fig. 7. The lower left corner of Fig. 6 is magnified to show effective permittivities of dilute mixtures.

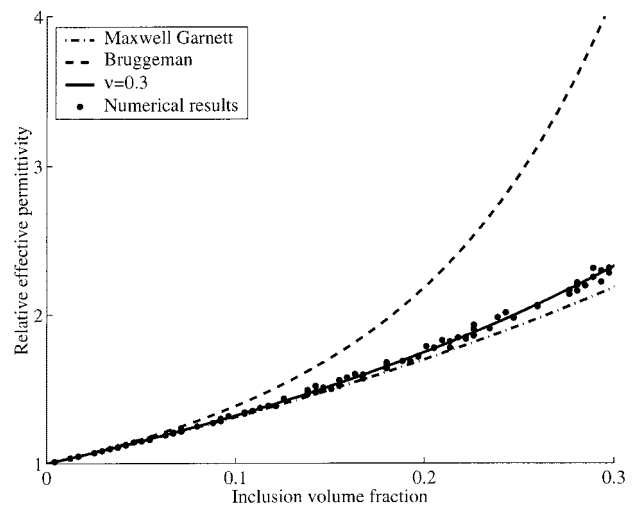


Fig. 9. Mixing models are plotted with numerical results for the raisin pudding mixture without clustering ($k = 51$).

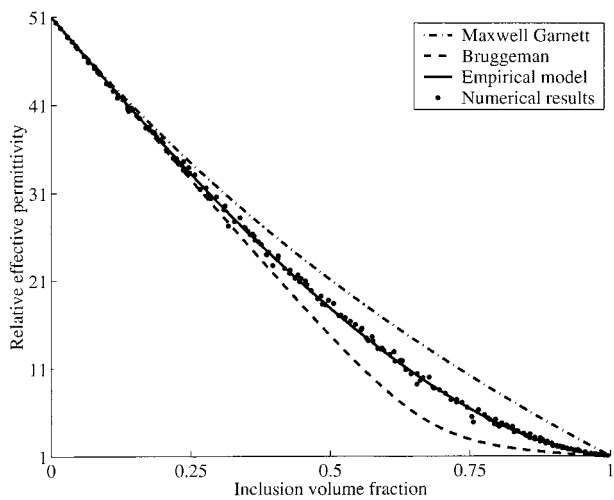


Fig. 8. Mixing models are plotted with numerical results for the Swiss cheese mixture ($k = 1/51$).

be restricted because even the maximum packing would have an inclusion volume fraction of only 0.74. In this study we modeled mixtures with volume fraction less than 0.3. During calculations it was found out that the results converged rather poorly when grid step size was reduced. A better convergence was found by using the minimum estimation of Fig. 3 rather than the average of limit estimations in the determination of local permittivity. The results showed that the effective permittivity values of the raisin pudding mixture were lower than in the clustered case (see Fig. 9). The ν -value seemed to be circa 0.3 which is rather close the Maxwell–Garnett model ($\nu = 0$). The ν -value of Swiss cheese mixture also came down and appeared to be about 1.3.

D. Field Distribution

From a discrete potential solution it is easy to calculate electric field as a gradient and electric flux by multiplying this field with local permittivity. The electric flux has a tendency to favor high permittivity materials. This is clearly seen in Figs. 10 and 11.

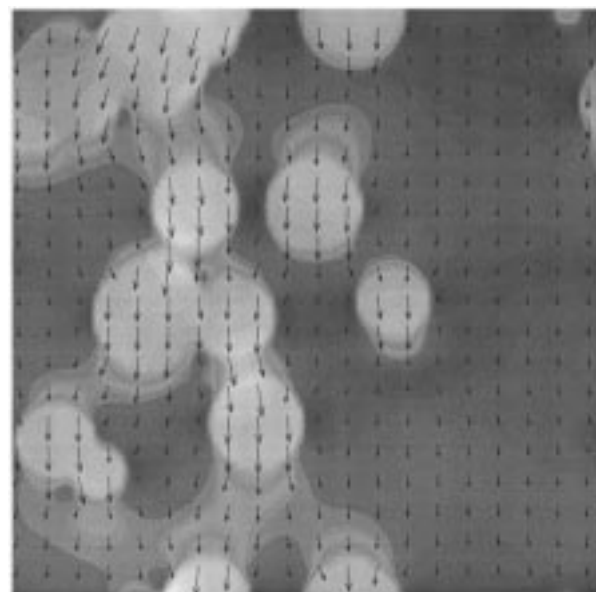


Fig. 10. Electric flux at the cross section of a random raisin pudding mixture ($\epsilon_i/\epsilon_e = 6$).

V. CONCLUSIONS

The reported technique offers the ability to study average characteristics of a random dielectric mixture. Naturally the calculated results agree well with theoretical models at low inclusion volume fractions. But at higher volume fraction values the effective permittivity seem to differ from models. A new mixing model based on numerical simulations is introduced.

One interesting result of this study was to realize that for dilute raisin pudding mixtures the Maxwell–Garnett prediction is acceptable when clustering is not allowed whereas the Bruggeman model is closer to the simulations when clustering is allowed. Comparing the results of 2-D mixtures [2] with the 3-D mixtures one can see that the overall effective permittivity distribution of 2-D mixtures is much wider than the distribution of 3-D mixtures. This is very natural because randomly placed parallel cylinders are more likely to connect together to form

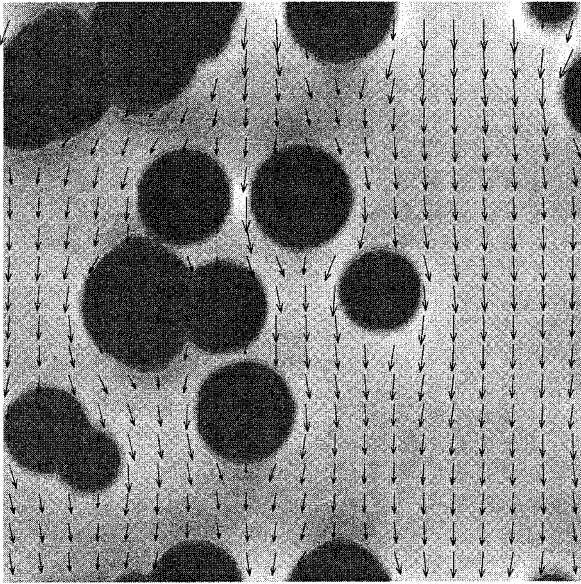


Fig. 11. Electric flux at the cross section of a random cheese mixture ($\epsilon_i/\epsilon_e = 1/6$).

special chain-like structures than randomly placed spheres. A common factor for 2-D and 3-D mixtures is that numerical results fall between the Maxwell–Garnett and the Bruggeman models in both cases.

The derivation of finite difference equations for electric potential is an essential issue. Random mixtures have numerous arbitrarily oriented material interfaces which are problematic to model in the discrete computation lattice. The technique based on the minimum and maximum limits of the local permittivity was used.

The introduced algorithm is straightforward and fast but still accurate enough to be used in the studies of random dielectric mixtures.

REFERENCES

- [1] O. Pekonen, K. Kärkkäinen, A. Sihvola, and K. Nikoskinen, "Numerical testing of dielectric mixing rules by FDTD method," *J. Electromagn. Waves Applicat.*, vol. 13, pp. 67–87, 1999.
- [2] K. Kärkkäinen, A. Sihvola, and K. Nikoskinen, "Effective permittivity of mixtures: Numerical validation by the FDTD method," *IEEE Trans. Geosci. Remote Sensing*, vol. 38, pp. 1303–1308, May 2000.
- [3] J. C. M. Garnett, "Colors in metal glasses and metal films," *Trans. R. Soc.*, vol. CCIII, pp. 385–420, 1904.
- [4] A. Sihvola and I. Lindell, "Polarizability modeling of heterogeneous media," in *Dielectric Properties of Heterogeneous Materials, PIER 6 Progress in Electromagnetics Research*, A. Priou, Ed. Amsterdam, The Netherlands: Elsevier, 1992, pp. 101–151.
- [5] D. A. G. Bruggeman, "Berechnung verschiedener physikalischer konstanten von heterogenen substanzen, i. dielektrizitätskonstanten und leitfähigkeiten der mischkörper aus isotropen substanzen," *Ann. Phys.*, vol. 24, no. 5, pp. 636–664, 1935.
- [6] D. Polder and J. H. van Santen, "The effective permeability of mixtures of solids," *Physica*, vol. 12, no. 5, pp. 257–271, 1946.
- [7] A. Sihvola, *Electromagnetic Mixing Formulas and Applications*, ser. IEE Electromagnetic Waves Series. London, U.K.: IEE, 1999.
- [8] W. E. Kohler and G. C. Papanicolaou, "Some applications of the coherent potential approximation," in *Multiple scattering and waves*, P. L. Kohler and G. C. Papanicolaou, Eds. New York: Wiley, 1981, pp. 199–223.
- [9] O. Wiener, *Zur theorie der refraktionskonstanten* Berichtüber die Verhandlungen Königlich-Sächsischen Gesellschaft der Wissenschaften zu Leipzig, vol. 62, 1910.
- [10] K. E. Atkinson, *An Introduction to Numerical Analysis*. New York: Wiley, 1988, ch. 2.



Kimmo Kärkkäinen (S'00) was born on February 1, 1973, in Kuopio, Finland. He received the Dipl. Eng. degree in 1998 and the Lic. Tech. degree in electrical engineering in 2000, both from Helsinki University of Technology, Espoo, Finland.

He is currently working as a Visiting Researcher in the Applied Electromagnetics Group at the University of Victoria, Victoria, BC, Canada. His main research interests include electromagnetic theory, numerical methods, and especially FDTD techniques.



Ari Sihvola (S'80–M'86–SM'91) was born on October 6, 1957, in Valkeala, Finland. He received the Dipl. Eng. degree in 1981, the Lic. Tech. degree in 1984, and the Dr. Tech. degree in 1987, all in electrical engineering, from the Helsinki University of Technology (HUT), Espoo, Finland.

Besides working for HUT and the Academy of Finland, he has been a Visiting Scientist in the Research Laboratory of Electronics of the Massachusetts Institute of Technology, Cambridge (1985–1986), the Pennsylvania State University, State College (1990–1991), Lund University, Sweden (1996), and the Swiss Federal Institute of Technology, Lausanne (2000–2001). Currently, he is Professor of Electromagnetics at HUT with interests in electromagnetic theory, complex media, materials modeling, remote sensing, and radar applications.

Dr. Sihvola is Vice Chairman of the Finnish National Committee of URSI. He also served as the Secretary of the 22nd European Microwave Conference, held in August 1992 in Espoo.



Keijo Nikoskinen (S'86–M'92) was born in Kaajaani, Finland, in 1962. He received the Dipl. Eng., Lic. Tech., and Dr. Tech. degrees, all in electrical engineering from Helsinki University of Technology, Espoo, Finland, in 1986, 1989, and 1991, respectively.

From 1991 to 1994, he was a Junior Scientist at the Academy of Finland. He is currently a Professor of Electromagnetics at HUT. His main professional interests are computational methods of electromagnetic field theory and antenna applications.